

## Article

# Recycling of Glass Fibers from Wind Turbine Blade Wastes via Chemical-Assisted Solvolysis

Maria Modestou <sup>1</sup>, Dionisis Semitekolos <sup>1</sup>, Tao Liu <sup>2</sup>, Christina Podara <sup>1</sup>, Savvas Orfanidis <sup>1</sup>, Ana Teresa Lima <sup>2</sup> and Costas Charitidis <sup>1,\*</sup>

<sup>1</sup> Research Lab of Advanced, Composite, Nano-Materials and Nanotechnology (R-NanoLab), School of Chemical Engineering, National Technical University of Athens, 9 Heroon Polytechniou, GR-15773 Athens, Greece; orfsavvas@chemeng.ntua.gr (S.O.)

<sup>2</sup> DTU Sustain, Department of Environmental and Resource Engineering, Technical University of Denmark, Brovej 118, 2800 Kongens Lyngby, Denmark

\* Correspondence: charitidis@chemeng.ntua.gr

## Abstract

Wind turbine blades (WTBs) have always been considered one of the greatest engineering achievements. They primarily use glass fiber-reinforced polymers (GFRPs) because of their lightweight nature, impressive strength-to-weight ratio, and durability. Until now, typical disposal methods of End-of-Life (EoL) WTBs are landfill or incineration. However, such practices are neither environmentally sustainable nor compliant with current regulations. This study investigates a low-temperature solvolysis process using a poly(ethylene glycol)/NaOH system under ambient pressure for efficient decomposition of the polyester matrix, promoting the potential of chemical recycling as an alternative to land-filling and incineration by offering a viable method for recovering glass fibers from WTB waste. A parametric study evaluated the influence of reaction time (4–5.5 h) and catalyst-to-resin ratio (0.1–2.0 g NaOH per g resin) on solvolysis efficiency. Optimal conditions (200 g PEG200, 12.5 g NaOH, 10 g GFRP, 5.5 h) achieved an ~80% decomposition efficiency and fibers exhibiting minimal surface degradation. SEM and EDX analyses confirmed limited morphological damage, while excessive NaOH (>15 g) caused notable etching of the glass fibers. ICP-OES of liquid residues detected high Na (780 mg/L) and Si (139 mg/L) concentrations, verifying partial dissolution of the fiber structure under strongly alkaline conditions. After applying a commercial sizing agent (Hydrosize HP2-06), TGA confirmed ~1.2% sizing mass, and nanoindentation analysis showed the interfacial modulus and hardness of re-sized fibers improved by over 70% compared to unsized recycled fibers, approaching the performance of virgin fibers.

**Keywords:** wind turbine blades; WTB; glass fiber reinforced polymer; GFRP; chemical recycling; solvolysis; low-temperature solvolysis; unsaturated polyester resin; UPR; sizing

Academic Editor: David P. Harper

Received: 8 October 2025

Revised: 25 November 2025

Accepted: 2 December 2025

Published: 5 December 2025

**Citation:** Modestou, M.; Semitekolos, D.; Liu, T.; Podara, C.; Orfanidis, S.; Lima, A.T.; Charitidis, C. Recycling of Glass Fibers from Wind Turbine Blade Wastes via Chemical-Assisted Solvolysis. *Fibers* **2025**, *13*, 163. <https://doi.org/10.3390/fib13120163>

**Copyright:** © 2025 by the authors. Licensee MDPI, Basel, Switzerland. This article is an open access article distributed under the terms and conditions of the Creative Commons Attribution (CC BY) license (<https://creativecommons.org/licenses/by/4.0/>).

## 1. Introduction

Undoubtedly, over the last few decades, composite materials have been extensively utilized in applications requiring lightweight structures combined with mechanical strength, particularly in sectors such as aerospace, automotive, and wind energy [1]. The widespread use of fiber-reinforced polymers within these sectors is continuously

expanding due to their energy-saving attributes and robust mechanical properties. However, the extensive quantities produced have necessitated serious consideration of their end-of-life management, as there are currently no standardized guidelines provided by any regulatory body regarding recycling or reuse methodology, aside from landfilling or incineration [2]. Particularly, this issue has emerged prominently in recent years, and the European Commission has notably highlighted the need for technologies to manage such materials at their life's end [3].

Recent developments have spurred extensive research, funded by the EU, focusing on recycling composite materials, particularly in the wind energy sector where old wind turbines, some over thirty years old, are reaching or have reached the end of their lifecycle [4]. Given the significant quantities involved, projected to reach approximately 43 million tonnes of blade waste worldwide by 2050 [4], these materials cannot simply be managed through landfilling or incineration; alternative, technologically innovative methods must be found [5,6]. There are few strategies that can extend the lifespan of composite material, such as repairing damaged components, through adhesive bonding or patch repairs [7,8], and reusing them in less critical applications, like pedestrian bridge designs [9], delaying the need for recycling. However, while efforts to delay recycling through repair or repurposing strategies may extend the lifecycle of composite materials, the need for recycling remains unavoidable in the long term.

The benefits of recycling such parts are substantial, since recycled fibers in optimal state could maintain most of their mechanical integrity, making them suitable for reuse in various applications, such as automotive [10] and construction [11,12]. This could reduce the environmental impact of producing virgin materials and enhance the sustainability of composite materials supply chain [13]. One such method is thermal recycling, also known as pyrolysis [14], a method proven effective, especially for the reclamation of glass fibers, since they are less prone to oxidation under the high temperatures compared to carbon fibers [15,16]. Nevertheless, it is an energy-inefficient process due to the significant energy input required to maintain these high temperatures, making it less environmentally and economically sustainable on a larger scale. In pyrolysis, FRPs are treated at high temperatures (typically between 500 and 600 °C) in an inert atmosphere, causing the polymeric matrix to decompose and leaving the fibers intact. At these temperatures, the mechanical integrity of the fibers is largely preserved. However, residual char may form on the fiber surface, due to incomplete decomposition of the polymer matrix. The presence of char can act as a physical barrier, reducing the interfacial adhesion with the new matrix when the fibers are reused [16,17]. Thus, further treatment is required through surface oxidation (between 450 °C and 600 °C) to remove it, while maintaining the fibers' tensile strength [14].

Another method is chemical recycling through solvolysis, utilizing solvents and catalysts in different conditions of temperature and pressure [18,19]. Chemical recycling involves the breakdown of polymers into mono-oligomers and the recovery of fibers from composites. While the fibers are successfully recovered, the mono-oligomers are often discarded as waste, primarily due to the solvents and catalysts used in the process [20].

Regarding solvolysis, the main processes, are taking place at low temperatures and ambient pressure, and at near- or supercritical conditions, offering a large number of possibilities due to a wide range of solvents, such as water, alcohols, acetone, glycols, or acids, and catalysts [5], which are used to break down the chemical bond of the polymer matrix, whether it is epoxy, polyester, or phenolic. Low-temperature solvolysis is typically performed below 200 °C and at atmospheric pressure. As a result, acids or bases, as well as catalysts, are required to break down the resin under mild circumstances. However, the properties of the reclaimed fibers can be negatively influenced by exposure to acids or bases during the recycling process [21]. On the other hand, sub- or super-critical solvolysis

is currently being investigated as an environmentally friendly, and sustainable process. However, it requires more complex and costly infrastructure due to the use of high pressure as a processing tool, rather than relying on catalysts. Sub- and super-critical fluids, such as water, acetone, and alcohol, serve as excellent reaction media for the decomposition of thermosets and can be recovered and reused, making the process more sustainable.

Previous research has explored the chemical recycling of composite materials using solvolysis with poly(ethylene glycol)/NaOH systems; however, these studies predominantly focused on the recycling of epoxy-based CFRPs. Specifically, Yang et al. [22] successfully recovered carbon fibers from epoxy-based CFRPs using a PEG/NaOH system at 200 °C. In contrast, the current research applies to a similar PEG/NaOH system specifically to GFRP wastes derived from wind turbine blades containing unsaturated polyester resin (UPR). Oliveux et al. also examined the chemical recycling of GFRPs with polyester resin matrices, employing subcritical water hydrolysis under elevated temperature and high-pressure conditions. However, their study focused on laboratory-prepared composites without additional additives typically present in actual wind turbine blades, nor did it investigate milder conditions at ambient pressure, as presented in the current work [19]. Mattsson et al. recycled End-of-Life wind turbine blades composed of GFRPs with unsaturated polyester resin, similar to the present research, but their process utilized sub- or supercritical water and alcohols under high-pressure conditions [6], differing from the low-temperature, catalyst-assisted approach presented here.

Recent studies emphasize hybrid recycling pathways that combine mechanical, thermal, and chemical treatments to optimize both energy consumption and fiber quality. For instance, Tao et al. [12] and Gonçalves et al. [11] demonstrated that incorporating recycled glass fibers into construction composites can reduce virgin material demand by up to 30%, while maintaining comparable mechanical performance. Likewise, Yousef et al. [23] recovered styrene-rich oils and intact fibers via controlled pyrolysis, offering potential for resin valorization. However, most of these routes rely on high-temperature processes ( $\geq 500$  °C) or limited mechanical reuse, raising concerns about their scalability and environmental footprint. In contrast, low-temperature solvolysis offers a promising and more sustainable alternative, enabling fiber recovery under mild conditions with reduced energy input and minimal emissions.

This work focuses on managing EoL WTB, particularly on the efficient recovery and reclamation of glass fibers. Initially, the blades were cut and shredded to reduce their size, making them manageable for further processing. Since the composition of the samples was unknown, a characterization of the composite materials was conducted using FT-IR spectroscopy and TGA to identify them. Following this, a parametric study of low-temperature solvolysis was performed, employing a poly(ethylene glycol)/NaOH system under ambient pressure. Specifically, the effects of reaction time, and the catalyst-to-resin ratio on the reaction efficiency were investigated. Finally, the reclaimed glass fibers were subjected to characterization techniques such as SEM, EDX, and TGA to evaluate their quality and the extent of resin removal. Application of a commercial sizing agent, followed by nanoindentation, restored the interfacial properties of composites by 70%.

## 2. Materials and Methods

### 2.1. Materials

WTB waste was sourced from landfills and supplied by A TEC (Goedersdorf, Austria), which also provided the shredder used in the process (Figure 1). Shredding was performed by PreZero (Barcelona, Spain) in a two-step process, by using a twin-shaft pre-shredder and then a crossflow shredder equipped with different screen sizes (60 mm, 40 mm, 20 mm, and 10 mm) to produce shredded material with a varied particle size distribution. The reagents used in the solvolysis experiments were Poly(ethelene Glycol) of a

M.W. of 200 (Sigma Aldrich—Saint louis, MO, USA) and Sodium Hydroxide (Sigma Aldrich—Saint louis, MO, USA) and Acetone (CoverPaints—Athens, Greece) as a cleaning solvent. Hydrosize HP2-06 (Michelman, Aubange, Belgium), a commercially available polymeric coating, was utilized for sizing the recycled fibers (rGFs). This sizing agent, comprising an anionic/nonionic phenoxy aqueous dispersion, improves fiber-matrix compatibility and thus enhances the mechanical properties of the resulting composites.



**Figure 1.** Photo of shredded composite WTB waste consisting of glass fiber reinforced polymer (**left**) and recycled glass fibers obtained from solvolysis (**right**).

## 2.2. Characterisation Methods

The composition of WTB waste was assessed using FT-IR, as no datasheets or related information were available for the materials. FT-IR spectroscopy was conducted using a Cary 630 spectrometer (Agilent, Santa Clara, CA, USA), which operates within a wavelength range of  $4000\text{--}400\text{ cm}^{-1}$  and has a resolution of  $4\text{ cm}^{-1}$ . Ten randomly selected WTB waste samples were analysed to determine their composition, for the material identification.

Optimal processing conditions, including temperature, time, and the amount of catalyst, for the effective decomposition of the polymer matrix and preservation of fiber integrity, were determined through TGA and SEM analysis. TGA was performed using a STA 449 F5 Jupiter (NETZSCH, Selb, Germany) apparatus to determine the resin content and thermal properties of the WTB wastes, as well as any resin residues on the recycled fibers. Analysis was conducted under an inert nitrogen ( $\text{N}_2$ ) atmosphere, with a scan rate of  $20\text{ K/min}$ . Three TGA measurements were conducted for three randomly selected WTB samples with particle sizes smaller than  $0.063\text{ mm}$ .

SEM was performed on the reclaimed fibers to assess any amount of residual resin after the recycling process and to evaluate fiber morphology, in order to optimize the process parameters, such as time, and catalyst quantity. Specifically, when residual resin was observed on the fibers, the reaction parameters were increased to enhance resin removal. Conversely, if fiber damage was evident, the parameters were adjusted downward to minimize mechanical degradation of the fibers. Additionally, EDX was used to identify the presence of resin residues on the recycled fibers. SEM analysis was carried out using a Hitachi TM3030 (Hitachi, Tokyo, Japan) tabletop microscope at magnifications up to  $\times 1000$ , equipped with a QUANTAX 70 EDX system, enabling the coupled analysis of chemical structure.

After solvolysis, the residual solution was collected and analyzed through Inductively Coupled Plasma-Optical Emission Spectrometry (ICP-OES) (Fisher Scientific, Waltham, MA, USA), calibrated for detecting metals and metalloids to assess whether the recycling process affects the integrity of the fibers and detect any residual inorganic components originating from the GFs in the liquid wastes. The eluates were tested for the presence of Al, As, Ba, Cd, Na, Pb, Sb, Se, Si, Sr, Ti, V, Zn, and Zr, to evaluate the composition

of the residual solution. The solution was diluted 100-fold (as shown in Figure 2), with three eluates obtained and analyzed per test series. Before analysis, samples were acidified with a few drops of nitric acid ( $\text{HNO}_3$ ) to ensure optimal ionization.

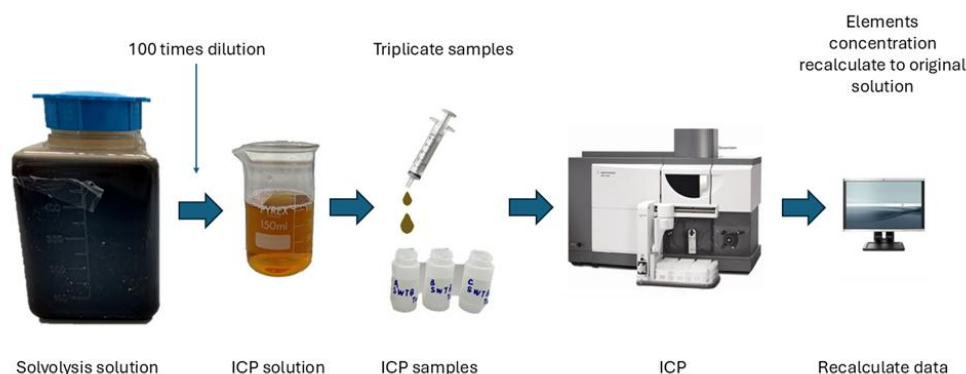


**Figure 2.** Workflow diagram of the ICP-OES testing procedure used to analyze the solvolysis liquid residues, including dilution, acidification, and elemental detection steps.

The ICP-OES setup utilized argon gas, with yttrium mixed with cerium as an internal standard to maintain quality assurance. The instrument operated with a plasma flow of 15.0 L/min, an auxiliary flow of 1.50 L/min, and a nebulizer pressure of 200 kPa. Sample uptake was delayed by 30 s, with a pump rate of 15 rpm and a rinse time of 20 s between samples. Each replicate was measured for 10 s, with an instrument stabilization delay of 17 s, and three replicates were taken per sample for accuracy.

The same TGA equipment was employed to confirm the successful application of the sizing agent, characterized by a slight mass loss occurring between 250 and 400 °C. Additionally, this analysis can evaluate the structural integrity of the fibers; any mass loss significantly exceeding the expected sizing-related amount indicates possible structural damage to the fibers. TGA measurements were performed under a nitrogen atmosphere at a flow rate of 50 mL/min, heating samples to 900 °C with a heating rate of 10 °C/min.

### 2.3. Solvolysis

The Poly(ethylene glycol)/NaOH system promotes glycolysis, a transesterification reaction that follows a nucleophilic substitution mechanism [24], facilitating the decomposition of the polyester matrix into oligomers with improved solubility in polar solvents. The presence of NaOH introduces hydroxyl anions, which attract the electrophilic centers of the ester bond, within the polymer chains. Nucleophilic substitution reactions involve a nucleophile attacking an electrophile to replace a leaving group (also known as. nucleofuge) [25], which, in this case, is facilitated by glycol (e.g., ethylene glycol, diethylene glycol, or polyethylene glycol). Polyethylene glycol with a molecular weight of 200 (PEG200) is particularly effective, as literature suggests it exhibits higher reactivity than PEGs of other molecular weights [22]. Transesterification catalysts, such as metal-based bases, are often employed to increase the reaction rate [26], enhancing the overall efficiency of polymer degradation.

As shown in Figure 3, under NaOH catalysis, PEG–O–nucleophiles attack ester carbonyls within the UPR network, affecting transesterification (glycolysis). This interaction results in the breakage of the polyester backbone and the formation of PEG-ester and hydroxyl-terminated oligomers, while decreasing the crosslink density and yielding soluble fragments [24].

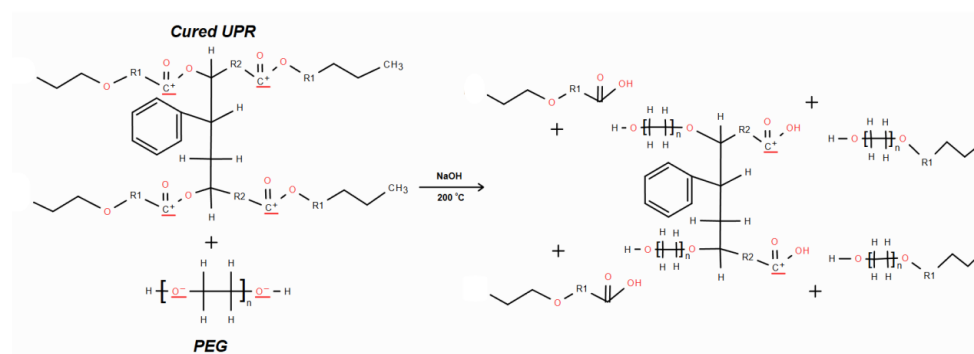


**Figure 3.** Chemical structures of the Unsaturated Polyester (Electrophilic) and PEG (Nucleophilic) (Left), Plausible reaction mechanism for solubilisation of Polyester Resin using PEG200/NaOH leading to the formation of soluble oligomers (Right).

Solvolysis on the WTB wastes was conducted, using a 500 mL three-necked round-bottomed flask with a reflux condenser and magnetic stirring, utilizing a Poly(ethylene glycol)/NaOH system at 200 °C at ambient pressure, varying parameters such as time, and composite waste and NaOH mass.

Table 1 summarizes the experimental parameters and conditions applied during the solvolysis experiments, including the quantities of PEG200, NaOH, and WTB waste, as well as the reaction time and stirring speed. The experimental investigation focused primarily on the amount of sodium hydroxide (NaOH) and the reaction time to identify the optimal conditions. The objective was to achieve maximum removal of residual resin from the fibers while minimizing fiber damage and mechanical degradation.

**Table 1.** Experimental Parameters and Conditions.

Exp.	Amount of PEG200 (gr)	Amount of NaOH (gr)	Amount of WTB Wastes (gr)	Reaction Time (Hours)	Stirring Speed (rpm)	Exp.
1	200	1	10	4	200	1
2	200	3	10	4	200	2
3	200	3	10	5.5	200	3
4	200	8	10	4	200	4
5	200	8	10	5.5	200	5
6	200	10	10	4	200	6
7	200	10	10	5.5	200	7
8	200	10	5	4	200	8
9	200	20	10	5.5	200	9
10	200	20	10	4	200	10
11	200	15	10	5.5	200	11
12	200	15	10	4	200	12
13	200	12.5	10	5.5	200	13
14	200	12.5	10	4	200	14

#### 2.4. Upscaling

The upscaling of the process was performed in a 10 L batch glass jacketed reactor also known as a double-walled reactor, consisting of an inner vessel (core) that holds the chemical reactants and a surrounding outer shell (jacket) that circulates a heating/cooling oil. This setup allows the temperature of the reactants to be controlled by regulating the temperature of the heat transfer fluid. The temperature of the reactants was maintained at 200 °C, consistent with the conditions used in the lab-scale setup.



Stirring and dosing are also critical components in the operation of jacketed lab reactors, as they help to ensure that the reactions within the reactor are efficient, effective, and safe. The reactor was equipped with mechanical stirring. To enable the scale-up to a 10 L batch reactor, the process was first scaled up to a 2 L reactor, also equipped with mechanical stirring. Observations indicated that a slightly reduced ratio of NaOH was necessary to achieve equivalent results. This adjustment was attributed to the transition to mechanical stirring, which provides higher torque and it is more effective for viscous or complex reactions where enhanced mixing power is required [27,28].

Due to the slower heating rate in the 10 L reactor, NaOH was introduced at three distinct elevated temperatures (80 °C, 120 °C, and 170 °C) to allow for better control of the reaction progression and exothermic behavior. Adding NaOH progressively, rather than all at once at the start, helped manage the reaction kinetics more effectively, by moderating the rate of polyester matrix breakdown and minimizing sudden heat release, and preventing the risk of thermal runaway.

By controlling the temperature of the medium in the jacket, the temperature of the reaction inside the reactor can be precisely controlled. To maintain a stable temperature profile, a side condenser was incorporated into the system to facilitate distillation. The condenser was installed to remove vapors that re-entered the inner vessel as droplets, lowering the reaction temperature.

As shown in Figure 4, the minor temperature oscillations observed between approximately 2200 and 7500 s correspond to the three NaOH dosing steps at 80, 120, and 170 °C. These short transients, lasting only a few minutes, are attributed to the heat of NaOH dissolution in PEG200, temporary viscosity and heat-transfer fluctuations, and the initial exothermic onset of the base-catalyzed transesterification reaction. The system's temperature control rapidly stabilized after each dosing event, maintaining a constant plateau around 200 °C for the remainder of the process. These variations are therefore operational rather than kinetic. The successful validation of the temperature profile and the effective control of the reaction kinetics allowed for further optimization of critical process parameters. This optimization resulted in a reduction in the overall reaction time to 5 h, while the stirring speed was decreased to 100 rpm, maintaining efficient mixing throughout the reaction.

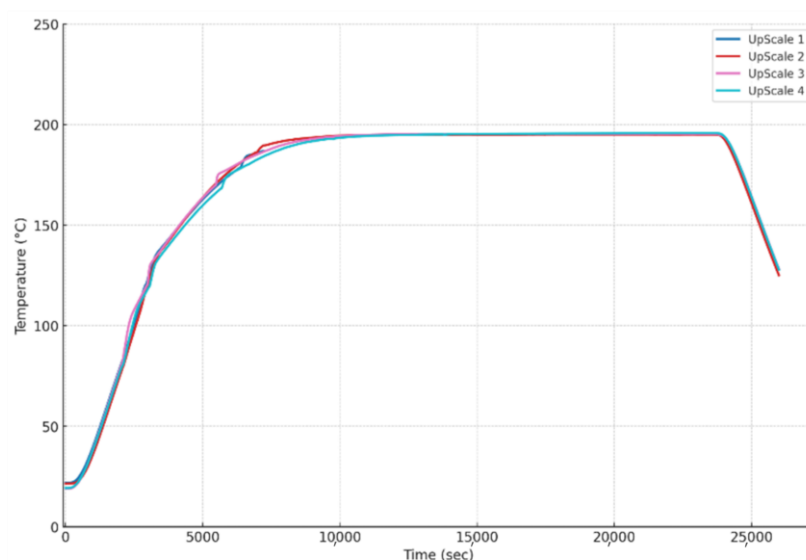


**Figure 4.** Temperature profile of the 10 L jacketed reactor during the scaled-up solvolysis process. The three NaOH dosing points (80 °C, 120 °C, 170 °C) and the stabilization plateau near 200 °C are indicated.

### 2.5. Fiber Treatment & Interface Assessment

Recycled glass fibers retrieved from the solvolysis process exhibit significantly low interfacial properties when integrated into new composite materials. This occurs due to the loss of original sizing agents and surface treatments during recycling, which impacts the effective adhesion between the fiber surfaces and the polymer matrix. The absence of appropriate sizing results in weak fiber-matrix interfaces, affecting the mechanical performance and structural integrity of the composite materials. To address this, a sizing agent was applied to the recycled GFs. Based on previous experimental experience [29], 20 mL of Michelman HP206 solution, was diluted to a concentration of 0.5% solids and applied per 5 g of recycled GFs to achieve adequate coverage and effective sizing. The selected concentration and volumes were established through preliminary trials to ensure uniform coating and optimal interfacial enhancement. The successful application of the sizing layer was validated by TGA, confirming the presence of the sizing material on the fiber surfaces.

To assess the interfacial properties, samples for nanoindentation were prepared using a grinding and polishing protocol. Initially, fibers were impregnated with epoxy resin and consolidated under tension to produce rigid samples suitable for mounting. Subsequently, these prepared samples were mounted in cylindrical molds (40 mm diameter) using a cold-mounting resin system.

After full curing, the mounted specimens underwent grinding and polishing steps on a QPOL grinding-polishing machine (ATM, Mammelzen, Germany). Grinding commenced with 320-grit abrasive paper until achieving a planar surface, followed by further grinding with 600-grit abrasive paper for one minute. Pre-polishing was then carried out using a 9  $\mu\text{m}$  diamond suspension for 5 min, followed by a 3  $\mu\text{m}$  diamond suspension for an additional 5 min. The final polishing step involved the use of colloidal silica suspension for 90 s to achieve a smooth and defect-free surface suitable for nanoindentation testing.

Nanoindentation was conducted using a FEMTO I-104 nanoindenter (FemtoTools AG, Buchs, Switzerland), using Continuous Stiffness Measurements and employing depth-controlled indentation with a maximum depth of 4 nm. The primary objective was to map mechanical property variations across areas containing individual glass fibers embedded within an epoxy matrix, characterizing the fiber-matrix interface behavior. Indentations were performed in grids consisting of 900 indentation points, arranged as  $30 \times 30$  matrices with an inter-indent spacing of 1  $\mu\text{m}$  and an averaging indent time of 2.5 s. Each indent location was positioned to ensure mechanical characterization across both fiber-rich regions and matrix-rich areas, capturing the local variations in mechanical properties.

Three distinct sample types were evaluated: reference fibers with original commercial sizing, recycled fibers retrieved through solvolysis without sizing, and sized recycled fibers subsequently coated with Michelman HP206 sizing solution. Figure 5 presents an optical micrograph of the polished cross-section of glass fibers embedded in an epoxy resin matrix. Two representative regions are indicated: Area 1 corresponds to a resin-only zone, which was used as a reference to determine the baseline nanomechanical properties of the pure matrix, while Area 2 highlights a single glass fiber embedded within the resin, used to evaluate the local mechanical response of the fiber and its surrounding interfacial region. This configuration allowed a direct comparison between the bulk matrix, the fiber, and the interphase properties obtained from nanoindentation mapping. Improved interfacial adhesion from sizing should appear as elevated values at the fiber-matrix interface compared to untreated recycled fibers. Observations from nanoindentation data thus facilitate direct correlation between the fiber surface treatments and resulting interfacial mechanical performance.





**Figure 5.** Optical micrograph of the polished cross-section of glass fibers embedded in an epoxy matrix, showing the nanoindentation test locations (Area 1, resin-only region and Area 2, region containing a single glass fiber, scale bar = 100  $\mu\text{m}$ ).

### 3. Results

#### 3.1. WTB Wastes Analysis

##### 3.1.1. Identification of WTB Waste Components

As presented in Figure 6, ten FT-IR spectra were obtained from randomly selected waste samples. No sample preparation was performed, resulting in inhomogeneity among the samples in terms of thickness and surface area. The band at  $1736\text{ cm}^{-1}$  confirms the presence of the  $\text{-C=O}$  ester group, while a strong peak at  $1260\text{ cm}^{-1}$ , attributed to the  $\text{-C-O-}$  bond of ester linkage, indicates the presence of polyester resin. More specifically the spectra display characteristic peaks associated with UPR [30,31]. Variations in transmittance intensities and slight shifts in the peaks are observed, which can be attributed to the non-uniformity of the samples and the possible presence of impurities.

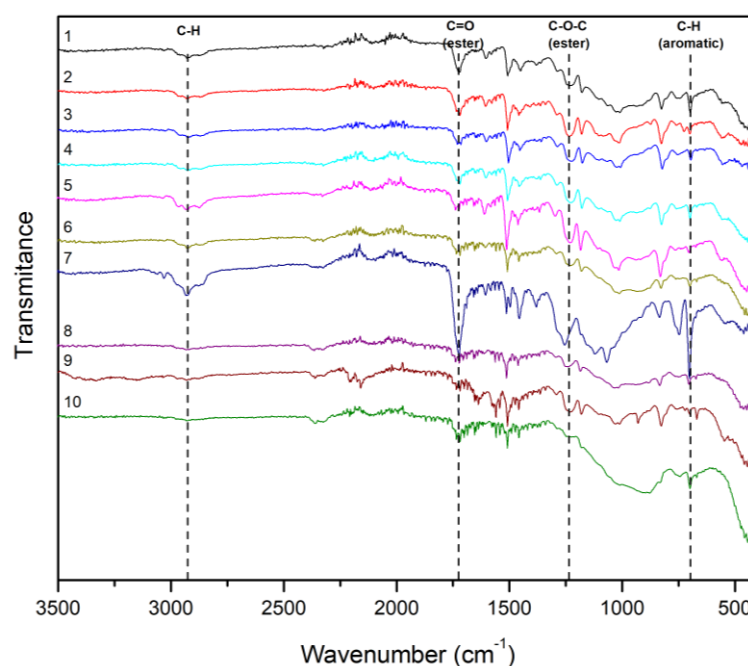


**Figure 6.** FT-IR spectra of ten randomly selected WTB waste samples, showing characteristic ester carbonyl peaks ( $1736\text{ cm}^{-1}$ ) and C–O–C ester linkage bands ( $1260\text{ cm}^{-1}$ ), confirming the presence of unsaturated polyester resin.

This finding aligns with earlier practices, as UPR was widely used in the manufacturing of early wind turbine blades. Consequently, EoL WTB composites predominantly consist of UPR [23,32]. However, in recent years, epoxy resins have largely replaced polyester and are now the most widely used matrices for wind blade composites due to their superior mechanical and thermal properties [33].

### 3.1.2. Thermal Properties of WTB & Fiber to Resin Weight Ratio

To investigate the thermal properties of GFRP waste, including its decomposition and weight loss behavior, TGA was carried out, and the results from the three experiments are presented in Figure 7.

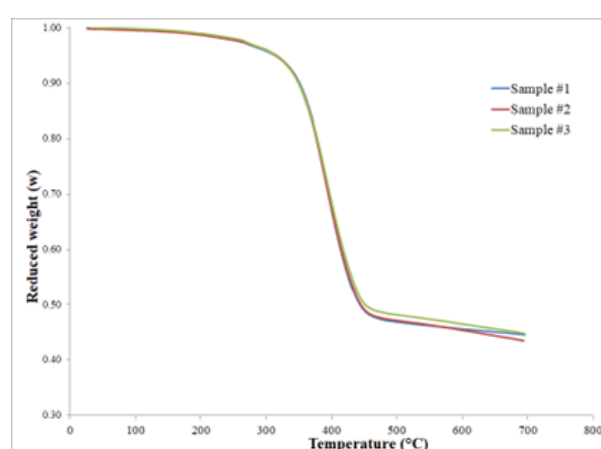


**Figure 7.** TGA curves of three representative WTB waste samples under  $\text{N}_2$  atmosphere showing ~55 % resin content.

The main decomposition peak, observed between  $300\text{ }^{\circ}\text{C}$  and  $500\text{ }^{\circ}\text{C}$  for all three samples, corresponds to the thermal degradation of the resin matrix [34]. The remaining mass, approximately 45%, is attributed to the thermally stable glass fibers, which remain intact within this temperature range [35]. Despite the inherent inhomogeneity of the initial material, the thermal degradation behaviour of the GFRP waste appeared to be relatively consistent during the inert atmosphere TGA analysis, exhibiting a resin content of approximately 55%.

### 3.2. rGFs and Solvolysis Liquid Wastes Analysis

#### 3.2.1. Decomposition Efficiency of Solvolysis

To investigate the thermal properties of recycled glass fibers and assess the decomposition efficiency of the solvolysis process, focusing on the amount of resin remaining on the fibers, TGA was performed on the experiments that showed the most promising results after an initial screening. The screening process excluded samples that were extremely fragile and prone to breaking upon touch, as well as samples that appeared rigid, indicating the presence of residual resin. Out of the 14 experiments conducted, experiments 1 through 6 exhibited visible residual resin due to an insufficient amount of NaOH, which limited the effective decomposition of the polyester resin. On the other hand, experiments 8 through 12 showed extreme fiber fragility because of excessive amounts of NaOH which after complete resin removal, further reacted with the silicate–aluminate network of the glass fibers (mainly  $\text{SiO}_2$  and  $\text{Al}_2\text{O}_3$  components), causing structural

degradation through the formation of soluble sodium silicates and aluminates, causing structural damage. As a result, TGA analysis was focused on Experiments 7, 13, and 14 to evaluate the decomposition efficiency under optimized conditions.

TGA curves presented in Figure 8 interpret a nearly 40% of residual resin on the fibers from Experiments 7 and 14, indicating incomplete decomposition. By contrast, the fibers reclaimed from Experiment 13 exhibited significantly reduced residual resin content, corresponding to a decomposition efficiency (Equation (1)) of approximately 80%. Although some resin remains on the fibers, the optimal conditions were identified in Experiment 13, which utilized 200 g of PEG200, 12.5 g of NaOH, and 10 g of GFRPs over a period of 5.5 h at 200 °C.

Moreover, the onset degradation temperature for the raw WTB wastes begins at approximately 350 °C, while the resin residue from the recycled fibers exhibits slightly lower onset temperatures (~250 °C). This suggests that the resin has been degraded during the solvolysis process, reducing its thermal stability and leading to expected losses at lower temperatures [36]. Additionally, the small weight losses observed after 300 °C in the reclaimed fibers are likely attributed to trapped solvent residues from post-processing, as the fibers were cleaned with water and acetone [37].

$$\text{Efficiency}(\%) = \frac{\text{Initial Resin}(\%) - \text{Residual Resin}(\%)}{\text{Initial Resin}(\%)} \times 100\% \quad (1)$$

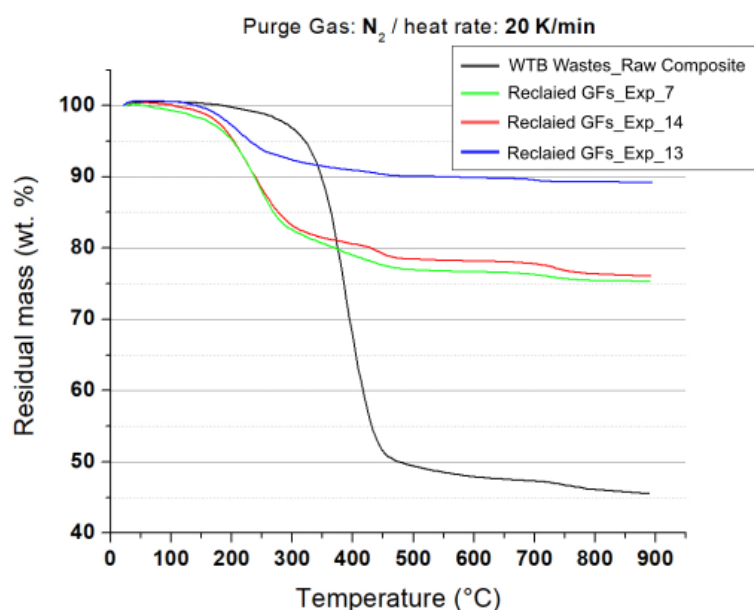


**Figure 8.** TGA analysis of raw WTB waste and recycled glass fibers from Experiments 7, 13, and 14, highlighting differences in residual resin content and thermal stability following solvolysis.

The decomposition efficiency achieved under mild solvolysis conditions of this work was compared with similar studies employing PEG/NaOH systems and sub- or super-critical routes. In epoxy-based composites, Yang et al. [38] reported decomposition efficiency up to 78% at 200 °C for 4 h using only 0.1 g NaOH per g composite under ambient pressure. By contrast, the treatment of EoL glass fiber–reinforced polyester systems typically requires a significantly higher catalyst-to-resin ratio (~1 g NaOH per g composite) to achieve comparable decomposition levels. This difference is mainly attributed to the resin chemistry: anhydride-cured epoxies are more susceptible to alkaline glycolysis than unsaturated polyester matrices, which contain styrenic crosslinks, inorganic fillers, and stabilizing additives that hinder solvent penetration and slow bond cleavage. Furthermore,

the aging and heterogeneity of industrial wind turbine blades can further reduce the efficiency of solvolysis, necessitating higher reagent loads and longer reaction times.

In related studies on end-of-life wind turbine blades summarized in Table 2, Mattsson et al. [6] investigated glycol- and alcohol-based solvolysis of UPR-GFRPs, reporting 50–85% resin degradation in ethylene/propylene glycol at 270 °C for 16 h, and 10–55% in water/1-propanol/KOH at 330 °C for 2–16 h, a two-step process reached ~75% resin removal efficiency. Although these processes required higher reaction temperatures than ambient-pressure systems, the extended treatment time and use of pressurized reactors enabled a more complete matrix breakdown and better control over fiber surface degradation. However, the elevated temperature and multi-step nature of the process increase energy demand and operational complexity, making it less favourable for large-scale recycling lines designed for continuous operation.

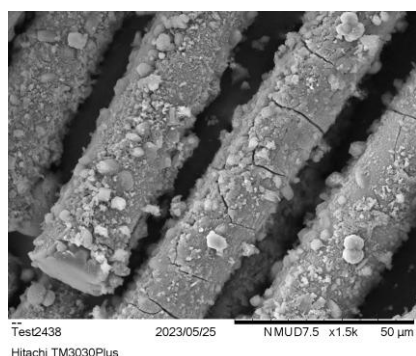
In comparison, sub- and supercritical solvolysis techniques, such as those demonstrated by Vogiantzi and Tserpes [39] who used supercritical water 400 °C and 300 bar, achieve 100% resin removal without the need for catalysts, while effectively preserving fiber integrity. The superior decomposition efficiency arises from the unique solvent properties of supercritical fluids, where reduced dielectric constant and enhanced diffusivity enable rapid penetration of the polymer network and cleavage of ester and ether bonds throughout the matrix. Despite these advantages, such processes require specialized high-pressure reactors and advanced control systems, representing a significant capital investment. Nevertheless, the combination of complete resin removal, high fiber quality, and solvent reusability positions supercritical solvolysis as a promising route for industrial-scale implementation of composite recycling in the near future.

**Table 2.** Comparison of decomposition efficiency of literature studies.

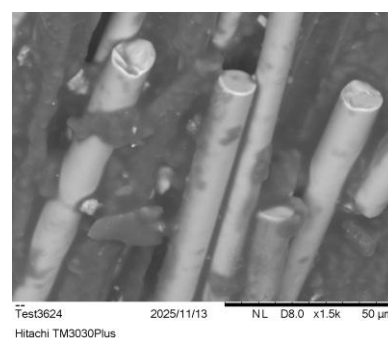
Citation	Method/Medium	Optimum Conditions	Decomposition Efficiency (%)	Resin/Fiber Type	Composite Type/Source
P. Yang et al. [38]	PEG/NaOH solvolysis	200 °C, 4 h, 0.1 g NaOH/g CFRP	~78	Epoxy-CF	Reference CFRP laminate
C. Mattsson et al. [6]	Ethylene glycon	270 °C, 16 h under pressure	~85	UPR-GF	EoL WTB waste
C. Vogiantzi & K. Tserpes [39]	Supercritical Water solvolysis	400 °C, 300 bar	~100	Epoxy-CF	Reference CFRP laminate

### 3.2.2. Morphological Characteristics of rGFs

Additionally, SEM and EDX were conducted on the reclaimed fibers to provide a visual representation of the TGA findings. Similarly to the TGA study, experiments 7, 13, and 14 were examined, along with Experiment 12 as a representative case, to observe the extent of fiber damage induced by NaOH, as presented in the SEM images in Figure 9.



(a)



(b)

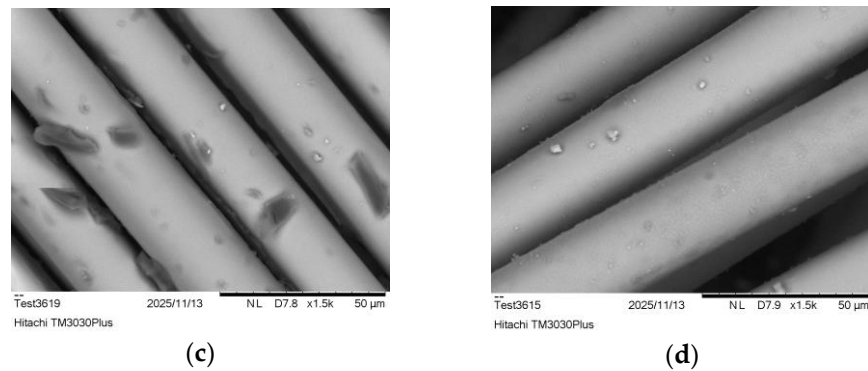
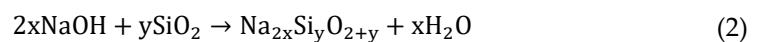


**Figure 9.** SEM micrographs of recycled glass fibers from (a) Exp 12, (b) Exp 7, (c) Exp 14, and (d) Exp 13. Images show varying degrees of fiber damage and residual resin. Scale bars = 50 µm.

Figure 9a displays the SEM images of Experiment 12, where the fibers appear extremely fragile and prone to breaking upon touch. This is clearly confirmed by the presence of cracks formed along the fiber surfaces. Such extensive damage occurred due to the excessive concentration of NaOH used in this experiment, which significantly weakened the fiber structure. It is important to note that while catalysts like NaOH assist in the recovery of fibers and the decomposition of the matrix, they simultaneously lead to fiber damage [40]. The degradation of the fibers is attributed to the reaction between the fibers, which are primarily composed of silicon dioxide ( $\text{SiO}_2$ ) [41], and the catalyst (NaOH). This reaction produces sodium silicate ( $x\text{Na}_2\text{O} \cdot y\text{SiO}_2$  or  $\text{Na}_{2x}\text{Si}_y\text{O}_{2y+x}$ ) as shown in the reaction below [42]:



This chemical interaction leads to the gradual degradation of the glass fibers during the recycling process, impacting the structural integrity of the recovered fibers.

Figure 9b,c corresponds to Experiments 7 and 14, respectively, where resin residues are clearly visible on the fiber surfaces. This observation aligns with the TGA results, which indicated approximately 40% residual resin content in these experiments, further confirming the incomplete decomposition of the polymer matrix under these conditions. The optimal case is observed in Figure 9d, where only minimal resin residues are present, as also indicated by the TGA results. This experiment yielded the cleanest fibers while simultaneously preserving an optimal fiber structure, ensuring their potential for reuse in new applications.

Figure 10 shows the corresponding EDX mapping for the respective cases shown in Figure 9. For the EDX mapping, silicon and carbon were selected as key elements, as silicon is the primary component of glass fibers [41], and carbon is predominantly found in the resin [29]. However, in Figure 10a Sodium was selected instead of silicon to highlight the high concentration of NaOH, alongside carbon for the resin. Sodium is represented in red on the mapping and is concentrated around the cracks, further confirming the excessive presence of NaOH, leading to the degradation of the fiber structure [40]. In Figure 10b,c, silicon is represented in red, while carbon appears in blue/light blue. As observed in both figures, resin residues are clearly visible, due to the carbon content, further confirming the TGA findings regarding the incomplete removal of the resin. In contrast, the EDX mapping in Figure 10d shows a significantly reduced presence of resin residues, as indicated by the minimal carbon content, represented in red, confirming that Experiment 13 achieved the best results in terms of resin removal.

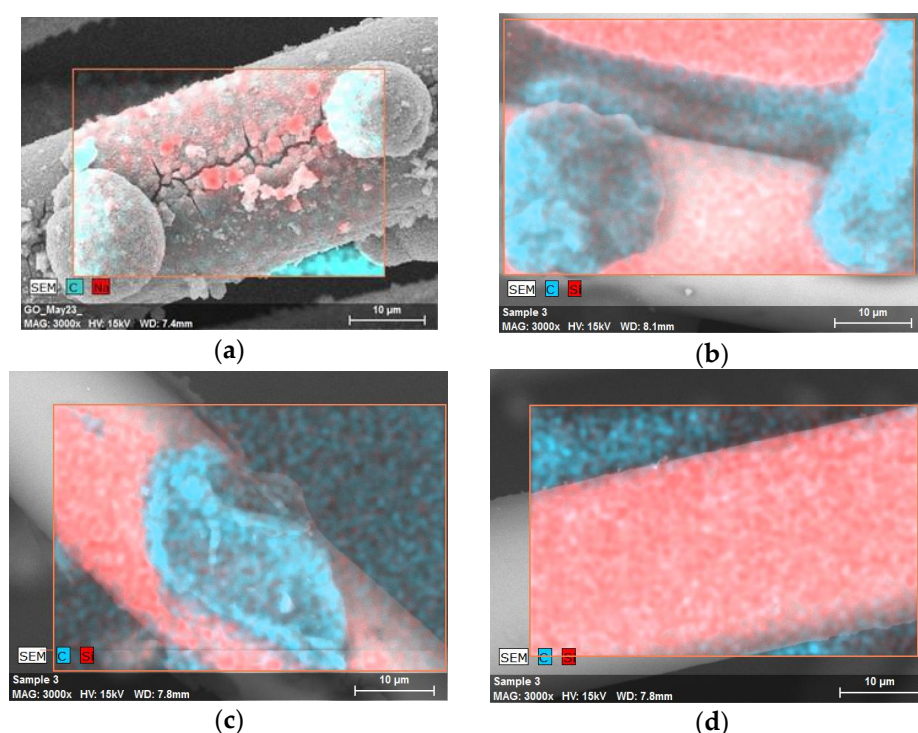


**Figure 10.** EDX elemental maps of recycled glass fibers from (a) Exp 12, (b) Exp 7, (c) Exp 14, and (d) Exp 13, corresponding to the SEM images in Figure 11. Images show varying degrees of fiber damage and residual resin. Scale bars = 10 µm.

### 3.2.3. Elemental Composition of Solvolysis Wastes

The ICP-OES analysis in Figure 11 reveals the elemental composition of the solvolysis solution from the chemical recycling of GFRP waste. The high concentration of silicon (138.62 mg/L) indicates significant degradation of the glass fibers, as confirmed by SEM images. This degradation originates from the alkaline attack of NaOH on the silicate–aluminate network of the E-glass fibers rather than on silicon dioxide alone. In such systems, NaOH can disrupt both Si–O–Si and Si–O–Al bonds, leading to the formation of soluble sodium silicates and aluminates and, consequently, to structural weakening of the fibers [40]. The presence of a considerable aluminium concentration (87.14 mg/L) further supports this mechanism, confirming that multiple oxides—mainly SiO<sub>2</sub> and Al<sub>2</sub>O<sub>3</sub>—participate in the dissolution process [41]. The notably high sodium level (780.7 mg/L) originates from the sodium hydroxide used as a catalyst in the solvolysis process, emphasizing its role in the decomposition of the composite matrix [22]. Lower concentration of titanium (3.34 mg/L) likely originates from protective coatings applied to enhance the mechanical properties of GFRPs, leveraging titanium’s superior hardness and wear resistance [43]. Similarly, the low zinc concentration (4.26 mg/L) can be attributed to anti-corrosion protective coatings [44,45]. The limited dissolution of these elements during solvolysis suggests they were less impacted by the process, possibly due to their inherent resistance to chemical degradation, as well as their relatively low initial concentrations in wind turbine blade. The detected antimony concentration (6.46 mg/L), along with other trace elements such as selenium, arsenic, barium, strontium, vanadium, zirconium, cadmium, and lead, is most plausibly attributed to environmental contamination from soil and surrounding landfill materials to which the WTB wastes were exposed [46–48].



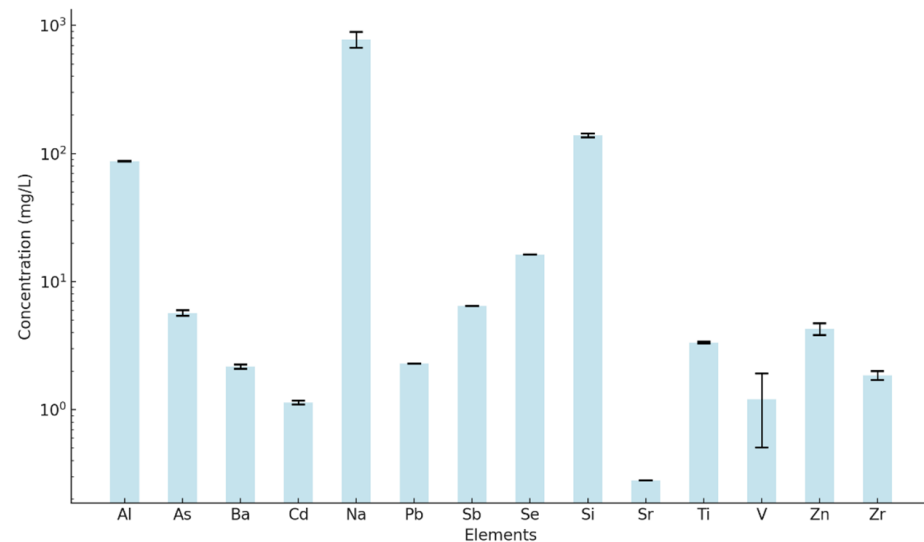


**Figure 11.** ICP-OES elemental analysis of the solvolysis liquid residues, showing concentrations of Na, Si, Al, Ti, Zn, Sb, and trace contaminants originating from glass fiber dissolution and environmental exposure of the WTB waste.

### 3.2.4. Sizing Confirmation

Figure 12 presents the TGA results for the optimally sized recycled glass fibers. Initially, the TGA curve displays a well-defined mass loss of approximately 1.2% occurring between 280 °C and 480 °C. This mass reduction is attributed to the thermal decomposition of the applied sizing agent, confirming the effective deposition of the Hydrosize® HP2-06 sizing layer. Such a temperature range for sizing decomposition aligns well with existing literature, where polymeric sizing agents typically degrade between 250 and 500 °C [49]. Subsequently, the stability and structural integrity of the recycled glass fibers were assessed by observing the mass profile up to 900 °C. No significant mass losses beyond the sizing decomposition range were observed. The stable mass profile confirms that the applied recycling conditions effectively removed the epoxy resin without compromising the intrinsic fiber structure, ensuring the mechanical integrity of the fibers is retained for subsequent composite applications. The stability and presence of sizing are critical, as these directly influence the interfacial adhesion and mechanical performance of the resulting composites.

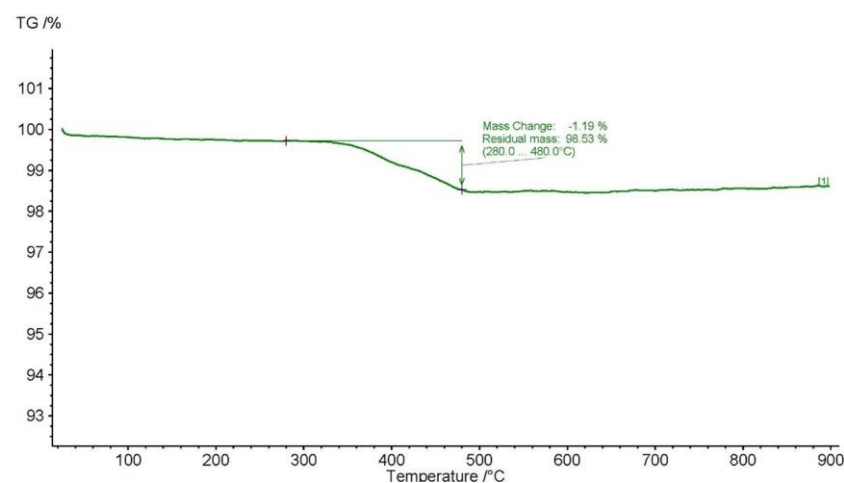




**Figure 12.** TGA curve of sized recycled glass fibers showing a characteristic ~1.2 % mass loss between 280 and 480 °C associated with the decomposition of the applied Hydrosized® HP2-06 sizing layer.

### 3.2.5. Interfacial Properties of rGFs

Figures 13–15 present the nanomechanical property maps of reduced modulus and hardness for the three types of GFs: reference fibers with commercial sizing, recycled fibers without sizing, and recycled fibers sized with Michelman HP206 solution. Additionally, reference measurements performed on regions containing only the epoxy matrix material were used as baseline points to interpret the fiber-related mechanical variations. Reduced modulus represents the local stiffness of the fiber-matrix interface under elastic deformation, combining the elastic properties of both the indenter and the sample material. Hardness, meanwhile, indicates resistance to plastic deformation under load, reflecting local material strength.

The nanoindentation mapping of the reference fibers (Figure 13) reveals consistently high and uniform values of both reduced modulus and hardness around the fiber-matrix interface, indicating good interfacial bonding and effective load transfer. The nanomechanical property maps demonstrate low variations, implying a well-integrated fiber-matrix interface where sizing promotes enhanced adhesion.

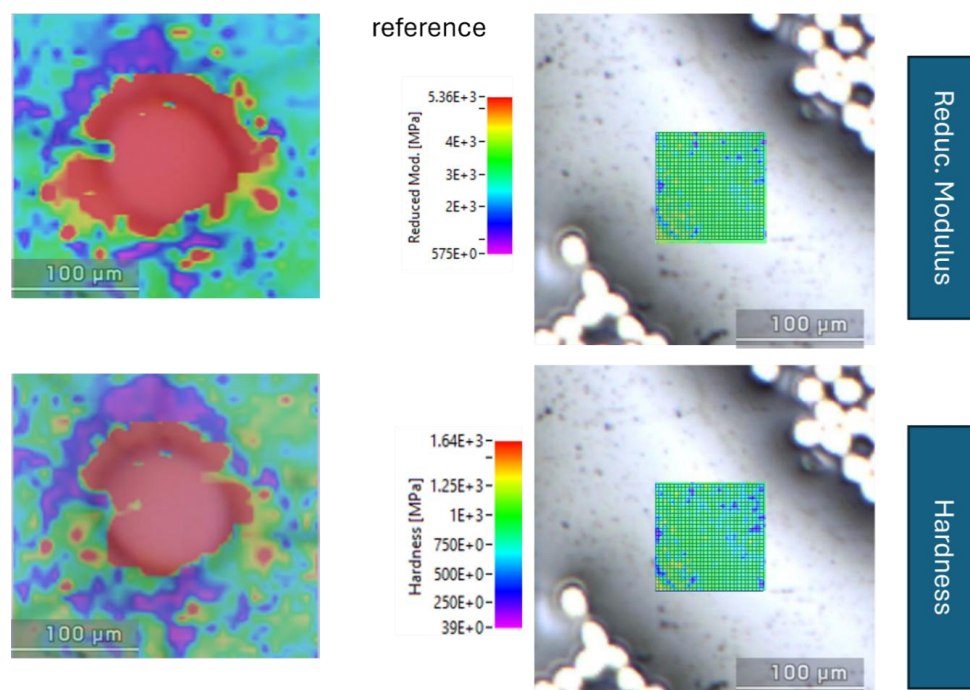


**Figure 13.** Nanomechanical properties' maps of reference glass fibers containing their original commercial sizing. Scale bar = 100 µm.

In sharp contrast, the recycled fibers without sizing (Figure 14) display a distinct reduction in both reduced modulus and hardness near the fiber surface. Such reduction indicates inadequate interfacial adhesion due to the absence of surface functional groups and sizing due to the chemical recycling, which significantly impairs the load-transfer capability between the fibers and matrix. The loss of these functional groups occurs during solvolysis, where aggressive chemical conditions (temperature, pressure, and/or reactive solvents and catalysts) cause hydrolytic cleavage of polymeric sizing layers and siloxane bonds from silane-based surface treatments. This leads to desilanization, stripping away

covalent and hydrogen bonds, thereby reducing local stiffness and promoting plastic deformation under indentation.

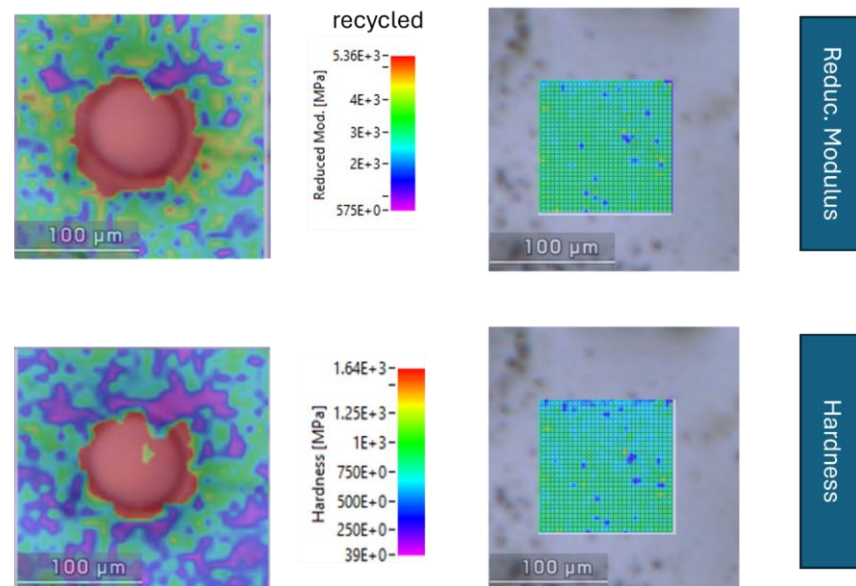


**Figure 14.** Nanomechanical properties' maps of recycled glass fibers without sizing. Scale bar = 100 µm.

The maps of sized recycled fibers (Figure 15) exhibit significant improvement in interfacial properties compared to the unsized recycled fibers. The reapplication of sizing agent increases both reduced modulus and hardness values at the interface, closely approaching the values obtained for the reference fibers. These elevated mechanical properties extend clearly beyond the immediate borders of the fiber, indicating the formation of a distinct interfacial region.

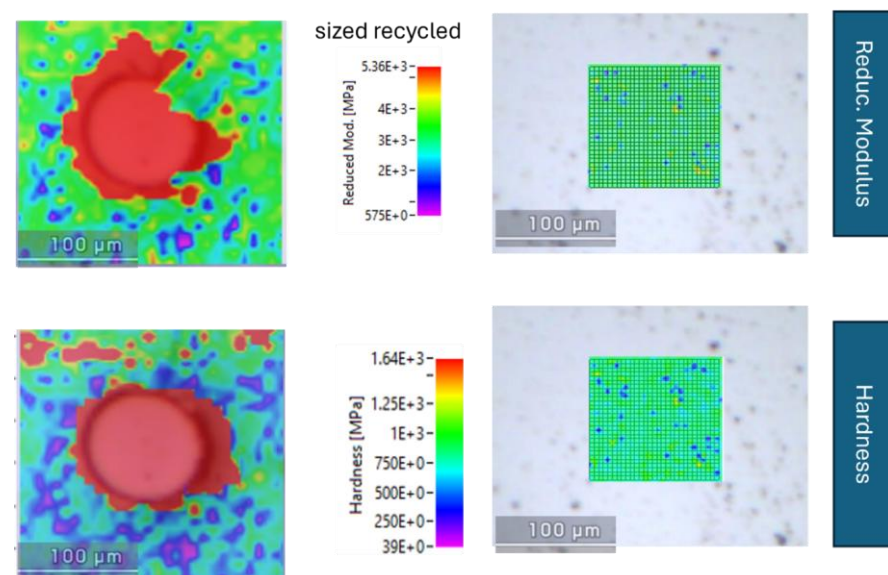


**Figure 15.** Nanomechanical properties' maps of recycled glass fibers after application of Hydrosizer® HP2-06 sizing. Scale bar = 100 µm.

The sizing mechanism improves compatibility and interfacial adhesion by forming chemical bonds, such as covalent and hydrogen bonds, as well as physical interactions like mechanical interlocking, between the fiber surface and the epoxy resin matrix. These

enhanced interactions create a robust interfacial region that extends the mechanical properties of the fibers outward into the surrounding matrix, with significantly improved stiffness and resistance to deformation compared to resin-only areas. This observation aligns with previous findings by Gu et al. [50], who demonstrated through nanoindentation mapping that an interphase region with a gradient of elevated stiffness extends beyond fiber boundaries, significantly enhancing local mechanical properties compared to the bulk resin.

Baseline measurements from matrix-only regions confirmed lower and relatively uniform mechanical property values, confirming that observed enhancements in nanomechanical properties are directly attributed to sizing effects at the fiber-matrix interface rather than variations within the matrix itself.

#### 4. Conclusions

This study aimed to develop and demonstrate a technologically feasible chemical recycling route for EoL WTBs through solvolysis under mild conditions of low temperature and ambient pressure. This approach was motivated by the growing environmental concern associated with the accumulation of GFRP waste and the lack of efficient, scalable recycling solutions. Initially, the composition of the WTB wastes was identified through FT-IR and TGA analyses, confirming the presence of unsaturated polyester resin as the main polymeric matrix, with a resin content of approximately 55%. This characterization step was essential for selecting the appropriate solvolysis system and tailoring the PEG/NaOH formulation to effectively decompose the resin matrix while preserving the structural integrity of the glass fibers. A parametric study was conducted to evaluate the influence of reaction parameters such as temperature, time, and NaOH concentration. Among the experimental conditions examined, the optimal results were obtained using 200 g PEG200, 12.5 g NaOH, and 10 g of GFRP waste at 200 °C for 5.5 h. Under these parameters, the TGA analysis revealed a decomposition efficiency of approximately 80%, indicating a significant removal of resin while maintaining satisfactory fiber integrity. SEM and EDX analyses provided information about the morphological and chemical characteristics of the recovered fibers. The images and elemental mappings confirmed minimal resin residues and negligible surface degradation under the optimized conditions, while higher NaOH concentrations resulted in fiber damage due to the formation of sodium silicates. Complementary, ICP-OES analysis of the solvolysis solution wastes verified the partial dissolution of glass fiber constituents at elevated NaOH contents, confirming the strong alkaline attack of NaOH on the silica network of the glass, which leads to the formation of soluble sodium silicates and subsequent weakening of the fiber structure. Following fiber recovery, the reapplication of sizing treatment was verified through TGA, which detected a characteristic mass loss between 280 and 480 °C associated with the decomposition of the sizing layer. Nanoindentation mapping further demonstrated that the re-sized recycled glass fibers exhibited substantially improved interfacial mechanical properties, approaching those of the reference commercially sized fibers. These results collectively confirm the potential of the applied recycling process to yield reusable fibers with restored surface functionality and mechanical compatibility for composite applications.

In conclusion, this study establishes an efficient low-temperature solvolysis method for recovering glass fibers from EoL WTBs, demonstrating a clear balance between decomposition efficiency and fiber preservation. The results also highlight the need to replace highly alkaline catalysts like NaOH with more sustainable solvent systems, such as water, alcohols, or acetone, under near- or supercritical conditions, promoting a more energy-efficient and environmentally responsible recycling pathway for GFRP structures.

## 5. Challenges & Future Recommendations

This study has encountered several challenges during the research process and has put emphasis on critical areas requiring attention for future investigations and industrial practices.

A primary challenge faced during this research was the lack of (composition) data related to EoL WTBs. This issue mainly arises due to the absence of standardized data tracking systems for composite materials throughout their lifecycle. To effectively manage EoL strategies and recycling processes, it is essential to apply advanced data management tools for new WTBs and other large-scale composite structures. The Digital Product Passport (DPP), as proposed by the European Union, represents a promising tool in this context, as it will provide detailed information about material compositions and lifecycle data. In addition, these tracking systems will aid recyclers in determining appropriate recycling methods and formulations.

Another significant challenge is the management and potential exploitation of liquid byproduct streams resulting from solvolysis processes. Given the substantial volumes of waste generated, it is crucial to explore innovative methods for their reuse or valorization. One potential alternative currently under investigation is utilizing these wastes as precursors for synthesizing nanomaterials through Chemical Vapor Deposition. This method could provide a viable solution to waste management and also create high-end secondary products, contributing to the sustainability and circularity of composite recycling practices.

**Author Contributions:** Conceptualization, M.M. and D.S.; methodology, M.M., T.L., S.O., C.P. and D.S.; investigation, M.M. and D.S.; writing—original draft preparation, M.M. and D.S.; writing—review and editing, D.S.; visualization, M.M.; supervision, C.C.; funding acquisition, A.T.L. All authors have read and agreed to the published version of the manuscript.

**Funding:** This work has been funded by European Union’s Horizon EU Innovation action project: “Recycle, Repurpose and reuse End-of-Life wind blade composites—A couple pre- and co-processing demonstration plant—Blades2Build” under the Grant Agreement No. 101096437, 10.3030/101096437.

**Data Availability Statement:** The original data presented in the study are openly available in Zenodo at <https://zenodo.org/records/17295153> (accessed on 1 December 2025).

**Conflicts of Interest:** The authors declare no conflicts of interest. The funders had no role in the design of the study; in the collection, analyses, or interpretation of data; in the writing of the manuscript; or in the decision to publish the results.

## References

1. Zhang, J.; Lin, G.; Vaidya, U.; Wang, H. Past, present and future prospective of global carbon fiber composite developments and applications. *Compos. Part B Eng.* **2023**, *250*, 110463. <https://doi.org/10.1016/j.compositesb.2022.110463>.
2. Majewski, P.; Florin, N.; Jit, J.; Stewart, R.A. End-of-life policy considerations for wind turbine blades. *Renew. Sustain. Energy Rev.* **2022**, *164*, 112538. <https://doi.org/10.1016/j.rser.2022.112538>.
3. European Commission, Directorate-General for Environment. “More Circular, Less Carbon: Chemical Recycling Holds Promise for Wind Turbine Blade Waste”, European Commission, Brussels, Science for Environment Policy—News Alert Service, Oct. 2023. Available online: [https://environment.ec.europa.eu/news/more-circular-less-carbon-chemical-recycling-holds-promise-wind-turbine-blade-waste-2023-10-19\\_en](https://environment.ec.europa.eu/news/more-circular-less-carbon-chemical-recycling-holds-promise-wind-turbine-blade-waste-2023-10-19_en) (accessed on 1 December 2025).
4. Liu, P.; Barlow, C.Y. Wind turbine blade waste in 2050. *Waste Manag.* **2017**, *62*, 229–240. <https://doi.org/10.1016/j.wasman.2017.02.007>.

5. Podara, C.; Termine, S.; Modestou, M.; Semitekolos, D.; Tsirogiannis, C.; Karamitrou, M.; Trompeta, A.-F.; Milickovic, T.K.; Charitidis, C. Recent Trends of Recycling and Upcycling of Polymers and Composites: A Comprehensive Review. *Recycling* **2024**, *9*, 37. <https://doi.org/10.3390/recycling9030037>.
6. Mattsson, C.; André, A.; Juntikka, M.; Tränkle, T.; Sott, R. Chemical recycling of End-of-Life wind turbine blades by solvolysis/HTL. *IOP Conf. Ser. Mater. Sci. Eng.* **2020**, *942*, 012013. <https://doi.org/10.1088/1757-899X/942/1/012013>.
7. Katnam, K.B.; Comer, A.J.; Roy, D.; da Silva, L.F.M.; Young, T.M. Composite Repair in Wind Turbine Blades: An Overview. *J. Adhes.* **2015**, *91*, 113–139. <https://doi.org/10.1080/00218464.2014.900449>.
8. Mishnaevsky, L. Repair of wind turbine blades: Review of methods and related computational mechanics problems. *Renew. Energy* **2019**, *140*, 828–839. <https://doi.org/10.1016/j.renene.2019.03.113>.
9. André, A.; Kullberg, J.; Nygren, D.; Mattsson, C.; Nedev, G.; Haghani, R. Re-use of wind turbine blade for construction and infrastructure applications. *IOP Conf. Ser. Mater. Sci. Eng.* **2020**, *942*, 012015. <https://doi.org/10.1088/1757-899X/942/1/012015>.
10. Meng, F.; McKechnie, J.; Pickering, S.J. An assessment of financial viability of recycled carbon fiber in automotive applications. *Compos. Part A Appl. Sci. Manuf.* **2018**, *109*, 207–220. <https://doi.org/10.1016/j.compositesa.2018.03.011>.
11. Gonçalves, R.M.; Martinho, A.; Oliveira, J.P. Evaluating the potential use of recycled glass fibers for the development of gypsum-based composites. *Constr. Build. Mater.* **2022**, *321*, 126320. <https://doi.org/10.1016/j.conbuildmat.2022.126320>.
12. Tao, Y.; Hadigheh, S.A.; Wei, Y. Recycling of glass fiber reinforced polymer (GFRP) composite wastes in concrete: A critical review and cost benefit analysis. *Structures* **2023**, *53*, 1540–1556. <https://doi.org/10.1016/j.istruc.2023.05.018>.
13. Pender, K.; Yang, L. Glass fiber composites recycling using the fluidised bed: A study into the economic viability in the UK. *CTR* **2023**, *3*, 221–240. <https://doi.org/10.3934/ctr.2023014>.
14. Termine, S.; Naxaki, V.; Semitekolos, D.; Trompeta, A.-F.; Rovere, M.; Tagliaferro, A.; Charitidis, C. Investigation of Carbon Fibers Reclamation by Pyrolysis Process for Their Reuse Potential. *Polymers* **2023**, *15*, 768. <https://doi.org/10.3390/polym15030768>.
15. Yang, T.; Dong, C.; Rong, Y.; Deng, Z.; Li, P.; Han, P.; Shi, M.; Huang, Z. Oxidation Behavior of Carbon Fibers in Ceramizable Phenolic Resin Matrix Composites at Elevated Temperatures. *Polymers* **2022**, *14*, 2785. <https://doi.org/10.3390/polym14142785>.
16. Oliveux, G.; Dandy, L.O.; Leeke, G.A. Current status of recycling of fiber reinforced polymers: Review of technologies, reuse and resulting properties. *Prog. Mater. Sci.* **2015**, *72*, 61–99. <https://doi.org/10.1016/j.pmatsci.2015.01.004>.
17. He, D.; Soo, V.K.; Stojcevski, F.; Lipiński, W.; Henderson, L.C.; Compston, P.; Doolan, M. The effect of sizing and surface oxidation on the surface properties and tensile behaviour of recycled carbon fiber: An end-of-life perspective. *Compos. Part A Appl. Sci. Manuf.* **2020**, *138*, 106072. <https://doi.org/10.1016/j.compositesa.2020.106072>.
18. Morin, C.; Loppinet-Serani, A.; Cansell, F.; Aymonier, C. Near- and supercritical solvolysis of carbon fiber reinforced polymers (CFRPs) for recycling carbon fibers as a valuable resource: State of the art. *J. Supercrit. Fluids* **2012**, *66*, 232–240. <https://doi.org/10.1016/j.supflu.2012.02.001>.
19. Oliveux, G.; Bailleul, J.-L.; Salle, E.L.G.L. Chemical recycling of glass fiber reinforced composites using subcritical water. *Compos. Part A: Appl. Sci. Manuf.* **2012**, *43*, 1809–1818. <https://doi.org/10.1016/j.compositesa.2012.06.008>.
20. Morici, E.; Dintcheva, N.T. Recycling of Thermoset Materials and Thermoset-Based Composites: Challenge and Opportunity. *Polymers* **2022**, *14*, 4153. <https://doi.org/10.3390/polym14194153>.
21. Dang, W.; Kubouchi, M.; Sembokuya, H.; Tsuda, K. Chemical recycling of glass fiber reinforced epoxy resin cured with amine using nitric acid. *Polymer* **2005**, *46*, 1905–1912. <https://doi.org/10.1016/j.polymer.2004.12.035>.
22. Yang, P.; Zhou, Q.; Yuan, X.-X.; Van Kasteren, J.M.N.; Wang, Y.-Z. Highly efficient solvolysis of epoxy resin using poly(ethylene glycol)/NaOH systems. *Polym. Degrad. Stab.* **2012**, *97*, 1101–1106. <https://doi.org/10.1016/j.polymdegradstab.2012.04.007>.
23. Yousef, S.; Eimontas, J.; Zakarauskas, K.; Striūgas, N. Recovery of styrene-rich oil and glass fibers from fibers-reinforced unsaturated polyester resin end-of-life wind turbine blades using pyrolysis technology. *J. Anal. Appl. Pyrolysis* **2023**, *173*, 106100. <https://doi.org/10.1016/j.jaap.2023.106100>.
24. Bartolome, L.; Imran, M.; Cho, B.G.; Al-Masry, W.A.; Kim, D.H. Recent Developments in the Chemical Recycling of PET. In *Material Recycling—Trends and Perspectives*; IntechOpen: London, UK, 2012. <https://doi.org/10.5772/33800>.
25. Shahrbabak, S.M.; Jalali, S.M.; Fathabadi, M.F.; Tayebi-Khorrami, V.; Amirinejad, M.; Forootan, S.; Saberifar, M.; Fadaei, M.R.; Najafi, Z.; Askari, V.R. Modified alginates for precision drug delivery: Advances in controlled-release and targeting systems. *Int. J. Pharm. X* **2025**, *10*, 100381. <https://doi.org/10.1016/j.ijpx.2025.100381>.
26. Achilias, D. Polymer Recycling Methods. In *Polymer Recycling*; Kallipos, Open Academic Editions: Athens, Greece, 2023. Available online: <https://repository.kallipos.gr/bitstream/11419/10205/1/164-ACHILIAS-Polymer-Recycling-CH02.pdf> (accessed on 1 December 2025).

27. Ameer, H.; Kamla, Y.; Sahel, D. Performance of Helical Ribbon and Screw Impellers for Mixing Viscous Fluids in Cylindrical Reactors. *ChemEngineering* **2018**, *2*, 26. <https://doi.org/10.3390/chemengineering2020026>.
28. Flores-Hernández, E.; Lira-Saldivar, R.; Acosta-Ortiz, R.; Méndez-Arguello, B.; García-López, J.; Díaz-Barriga-Castro, E.; González-Torres, A.; García-Carrillo, M. Synthesis and Characterization of Calcium Phosphate Nanoparticles and Effect of the Agitation Type on Particles Morphology. *Rev. Mex. Ing. Quim.* **2019**, *19*, 284–298. <https://doi.org/10.24275/rmiq/mat523>.
29. Semitekolos, D.; Terzopoulou, S.; Zecchi, S.; Marinis, D.; Farsari, E.; Amanatides, E.; Sajdak, M.; Sobek, S.; Smok, W.; Tański, T.; et al. Performance Restoration of Chemically Recycled Carbon Fibers Through Surface Modification with Sizing. *Polymers* **2024**, *17*, 33. <https://doi.org/10.3390/polym17010033>.
30. Koto, N.; Soegijono, B. Effect of Rice Husk Ash Filler of Resistance Against of High-Speed Projectile Impact on Polyester-Fiber-glass Double Panel Composites. *J. Phys. Conf. Ser.* **2019**, *1191*, 012058. <https://doi.org/10.1088/1742-6596/1191/1/012058>.
31. Chukwu, M.N.; Madueke, C.I.; Ekebafé, L.O. Effects of Snail Shell as Filler on the Mechanical Properties of Terephthalic Unsaturated Polyester Resin. *Niger. Res. J. Chem. Sci.* **2019**, *6*, 21–32.
32. Mishnaevsky, L.; Branner, K.; Petersen, H.N.; Beauson, J.; McGugan, M.; Sørensen, B.F. Materials for Wind Turbine Blades: An Overview. *Materials* **2017**, *10*, 11. <https://doi.org/10.3390/ma10111285>.
33. Reis, J.M.L.D.; Jurumenh, M.A.G. Experimental investigation on the effects of recycled aggregate on fracture behavior of polymer concrete. *Mat. Res.* **2011**, *14*, 326–330. <https://doi.org/10.1590/S1516-14392011005000060>.
34. Bansal, R.K.; Mittal, J.; Singh, P. Thermal stability and degradation studies of polyester resins. *J. Appl. Polym. Sci.* **1989**, *37*, 1901–1908. <https://doi.org/10.1002/app.1989.070370713>.
35. Fei, B. 2-High-performance fibers for textiles. In *Engineering of High-Performance Textiles*; Miao, M., Xin, J.H., Eds.; The Textile Institute Book Series; Woodhead Publishing: Cambridge, UK, 2018; pp. 27–58. <https://doi.org/10.1016/B978-0-08-101273-4.00002-0>.
36. Pączkowski, P.; Puszka, A.; Gawdzik, B. Investigation of Degradation of Composites Based on Unsaturated Polyester Resin and Vinyl Ester Resin. *Materials* **2022**, *15*, 1286. <https://doi.org/10.3390/ma15041286>.
37. Wiss, J.; Schmuck, J.-L. Cleaning validation using thermogravimetry. *J. Therm. Anal. Calorim.* **2010**, *104*, 315–321. <https://doi.org/10.1007/s10973-010-1144-7>.
38. Yang, P.; Zhou, Q.; Li, X.; Yang, K.; Wang, Y. Chemical recycling of fiber-reinforced epoxy resin using a polyethylene glycol/NaOH system. *J. Reinf. Plast. Compos.* **2024**, *33*, 2106–2114. <https://doi.org/10.1177/0731684414555745>.
39. Vogiantzi, C.; Tserpes, K. A Preliminary Investigation on a Water- and Acetone-Based Solvolysis Recycling Process for CFRPs. *Materials* **2024**, *17*, 1102. <https://doi.org/10.3390/ma17051102>.
40. Bashir, S.T.; Yang, L.; Liggat, J.J.; Thomason, J.L. Kinetics of dissolution of glass fiber in hot alkaline solution. *J. Mater. Sci.* **2018**, *53*, 1710–1722. <https://doi.org/10.1007/s10853-017-1627-z>.
41. Buschow, K.H.J. *Encyclopedia of Materials: Science and Technology*; Elsevier: Amsterdam, The Netherlands, 2001.
42. Rungrodnimitchai, S.; Phokhanusai, W.; Sungkhaho, N. Preparation of silica gel from rice husk ash using microwave heating. *J. Met. Mater. Miner.* **2009**, *19*, pp. 45–50. Available online: <https://jmmm.material.chula.ac.th/index.php/jmmm/article/view/235> (accessed on 23 July 2025).
43. Satishkumar, P.; Kumar, R.; Tripathi, N.M.; Sharma, A.; Desai, D.J.; Verma, A.; Natarajan, N.; Babbar, A. Integrating Titanium Coating with 3D-Printed GFRP Panels: An Innovative Approach to Harnessing Composite Strengths in Engineering Applications. In *Advances in Pre- and Post-Additive Manufacturing Processes*; CRC Press: Boca Raton, FL, USA, 2024.
44. Ding, R.; Zheng, Y.; Yu, H.; Li, W.; Wang, X.; Gui, T. Study of water permeation dynamics and anti-corrosion mechanism of graphene/zinc coatings. *J. Alloys Compd.* **2018**, *748*, 481–495. <https://doi.org/10.1016/j.jallcom.2018.03.160>.
45. Pop, A.B.; Iepure, G.; Titu, A.M.; Ravai-Nagy, S. Characterization and Corrosion Behavior of Zinc Coatings for Two Anti-Corrosive Protections: A Detailed Study. *Coatings* **2023**, *13*, 1460. <https://doi.org/10.3390/coatings13081460>.
46. Investing News Network. “Lesser Known, Yet Highly Critical”. September 2024. Available online: <https://investing-news.com/antimony-lesser-known-yet-highly-critical/> (accessed on 1 December 2025).
47. He, Y.; Xiang, Y.; Zhou, Y.; Yang, Y.; Zhang, J.; Huang, H.; Shang, C.; Luo, L.; Gao, J.; Tang, L. Selenium contamination, consequences and remediation techniques in water and soils: A review. *Environ. Res.* **2018**, *164*, 288–301. <https://doi.org/10.1016/j.envres.2018.02.037>.
48. Boudia, L.; Rafatullah, M.; Kerrouche, A.; Qutob, M.; Alosaimi, A.M.; Alorfi, H.S.; Hussein, M.A. A Review on Cadmium and Lead Contamination: Sources, Fate, Mechanism, Health Effects and Remediation Methods. *Water* **2022**, *14*, 3432. <https://doi.org/10.3390/w14213432>.

49. Li, Y.-F.; Hung, J.-Y.; Syu, J.-Y.; Chen, S.-H.; Huang, C.-H.; Chang, S.-M.; Kuo, W.-S. Effect of the Sizing Removal Methods of Fiber Surface on the Mechanical Performance of Basalt Fiber-Reinforced Concrete. *Fibers* **2024**, *12*, 10. <https://doi.org/10.3390/fib12010010>.
50. Gu, Y.; Li, M.; Wang, J.; Zhang, Z. Characterization of the interphase in carbon fiber/polymer composites using a nanoscale dynamic mechanical imaging technique. *Carbon* **2010**, *48*, 3229–3235. <https://doi.org/10.1016/j.carbon.2010.05.008>.

**Disclaimer/Publisher's Note:** The statements, opinions and data contained in all publications are solely those of the individual author(s) and contributor(s) and not of MDPI and/or the editor(s). MDPI and/or the editor(s) disclaim responsibility for any injury to people or property resulting from any ideas, methods, instructions or products referred to in the content.